Fluorescence Spectral Changes During the Folding of Intestinal Fatty Acid Binding Protein†

Ira J. Ropson* and Paula M. Dalessio

Department of Biochemistry and Molecular Biology, The Pennsylvania State University College of Medicine, Hershey, Pennsylvania 17033

Received December 5, 1996; Revised Manuscript Received May 12, 1997⊗

ABSTRACT: Although large changes in fluorescence intensity are observed during the folding and unfolding of many proteins, it has been difficult to associate these changes with specific structures or with the environmental changes which a particular tryptophan may undergo during these processes. The fluorescence spectral changes that occur during the folding and unfolding of rat intestinal fatty acid binding protein (IFABP) are described here. The intermediate observed during unfolding had spectral characteristics similar to those of unfolded protein, but with somewhat higher intensity. Stopped-flow circular dichroism measurements during unfolding showed that little if any secondary structure was associated with this intermediate. During refolding, the initial fluorescence spectrum was not that of native or unfolded IFABP, suggesting that some structure with intermediate fluorescent properties had formed during the deadtime of mixing. The shape and intensity of this initial spectrum were dependent on the final urea concentration, becoming more native-like at lower final concentrations of denaturant. A simple model for refolding suggests that a portion of the protein molecules obtain native structure and fluorescent characteristics during the deadtime of mixing, and that the remaining protein molecules have spectral characteristics similar to those of the intermediate observed during unfolding. Lower final concentrations of denaturant cause a larger proportion of molecules to follow the rapid refolding pathway. Knowledge of the fluorescence spectral characteristics of the intermediates formed during the folding and unfolding of any protein will improve our understanding of the nature of these structures.

The mechanism by which the amino acid sequence of a protein encodes the final tertiary structure remains one of the most difficult problems in biochemistry [reviewed by Matthews (1993), Ptitsyn (1996), and Creighton et al. (1996)]. Although an unstructured polypeptide has a very large number of potential conformations, the folding of a protein still occurs in a short period of time. As such, preferred intermediate states or paths for folding must exist in order for proteins to avoid searching through all the conformations available (Levinthal, 1968). The study of intermediates during folding is extremely difficult, since they do not usually accumulate to significant concentrations at equilibrium under physiological conditions (Matthews, 1993; Frieden et al., 1993; Engelhard & Evans, 1996). As such, much effort has been devoted to stopped-flow kinetic experiments, where a rapid change in solution conditions causes a change in the structure of the protein. The change in structure is observed by various optical or chemical quenching techniques (Frieden et al., 1993; Engelhard & Evans, 1996). However, this type of experiment typically reports only on global quantities, showing that a change in structure has occurred and/or that intermediates might be present, but do not identify the particular residues or structures involved (Frieden et al., 1993; Engelhard & Evans, 1996). The combination of stopped-flow techniques with hydrogen−deuterium exchange measurements has allowed the determination of when specific hydrogen bonds involved in secondary structure are formed during folding for a few proteins [reviewed by Englander and Mayne (1992), Baldwin (1993), and Englander (1993)]. However, only those proteins for which amide proton nuclear magnetic resonance (NMR)[1] assignments are available can be studied. Further, the NMR measurements do not report on the changes in environments of the amino acid side chains during the folding process.

Recent theoretical studies have emphasized the potential importance of hydrophobic interactions of these amino acid side chains both as the major driving force for folding (Dill, 1990; Rose & Wolfenden, 1993) and for the formation of folding initiation structures (Dill et al., 1993, 1995). Since tryptophan is a large hydrophobic amino acid, and is primarily responsible for the fluorescence of proteins, stopped-flow fluorescence experiments have been used to examine the change in hydrophobic side chain environments during folding. These experiments have shown that intermediates are indeed present on the folding pathway of many proteins (Frieden et al., 1993). However, it has not been possible to associate overall fluorescence intensity changes with specific structures or even with a change in the solvent exposure of a particular tryptophan during the transition (Engelhard & Evans, 1996). This paper describes the changes in the tryptophan fluorescence spectra that occur during the folding and unfolding of rat intestinal fatty acid binding protein (IFABP).

IFABP belongs to a family of small intracellular hydro-

† This work was supported by the National Science Foundation through Grant MCB 94-05282.

* Author to whom correspondence should be addressed.

⊗ Abstract published in *Advance ACS Abstracts,* July 1, 1997.

[1] Abbreviations: CD, circular dichroism; IFABP, rat intestinal fatty acid binding protein; EDTA, ethylenediaminetetraacetic acid; NMR, nuclear magnetic resonance; NATA, *N*-acetyltryptophanamide; NBS, *N*-bromosuccinimide.

S0006-2960(96)02983-2 CCC: $14.00

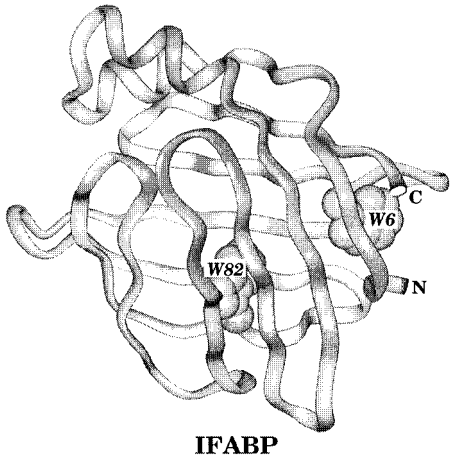

FIGURE 1: Ribbon drawing showing the backbone tracing and the sequence location of the two tryptophans of IFABP.

phobic-ligand binding proteins (Gordon et al., 1991; Veerkamp & Maatman, 1995; LaLonde et al., 1994). The crystal structure of apo-IFABP has been solved to 1.2 Å resolution (Scapin et al., 1992). The primary structural feature is two orthogonal β-sheets of five strands each (Figure 1). IFABP has no cysteines or prolines, thereby avoiding the folding complications associated with those residues. Previous studies on the folding and unfolding of this protein using chemical denaturants have shown that no significant concentrations of intermediates are found at equilibrium by fluorescence, CD, or absorbance measurements. However, at least one transient intermediate was detected by stopped-flow fluorescence measurements during both unfolding and refolding of this protein using guanidine hydrochloride as a denaturant (Ropson et al., 1990). However, those data could not determine which region(s) of the protein was (were) responsible for the observed fluorescence changes.

CD in the far-UV has been used to measure secondary structure content in proteins since the spectra can be deconvoluted to obtain information on α-helical, β-sheet, and turn content (Johnson, 1988). Recent advances in both CD and stopped-flow instrumentation have allowed the folding of some proteins to be studied by stopped-flow CD (e.g., Kuwajima et al., 1987, 1988; Mo et al., 1991; Sugawara et al., 1991). Preliminary studies by stopped-flow CD have shown that the fluorescence intermediate observed during the unfolding of IFABP with guanidine hydrochloride may have little if any secondary structure associated with it (Ropson et al., 1992).

This paper reports the fluorescence spectral changes that occur during the folding and unfolding of this protein, and confirms the lack of secondary structure associated with one of these intermediates by stopped-flow CD using a different denaturant.

MATERIALS AND METHODS

Sample Preparation. Intestinal fatty acid binding protein (IFABP) was produced in *Escherichia coli* and purified to homogeneity, and endogenous ligands were removed as previously described (Sacchettini et al., 1990). Protein purity was demonstrated by the presence of a single band on SDS and native polyacrylamide gels after electrophoresis. An extinction coefficient of 1.1 mg^{-1} cm^{-1} at 280 nm was used to determine IFABP concentration (Ropson et al., 1990).

Reagents. Denaturant stock solutions (10 M urea) used in unfolding and refolding experiments were prepared by dissolving ultrapure urea (Amresco) in distilled, deionized water. The urea solution was deionized by stirring for 1 h at room temperature following addition of 1 g of mixed-bed resin (Bio-Rad AG501-X8) per 150 g of urea. This urea stock solution was filtered through a 0.47 μm Whatman nylon membrane, divided into aliquots, and stored at −20 °C. Denaturant concentrations were determined by refractive index measurements employing a Milton Roy Abbe-3C refractometer at 25 °C in conjunction with equations relating refractive index to concentration (Pace, 1986). All experimental buffers contained 75 mM NaCl, 0.1 mM EDTA, and 25 mM sodium phosphate (pH 7). Buffers were filtered through a 0.22 μm membrane before use. Unless otherwise denoted, all chemicals were reagent grade.

Stopped-Flow Fluorescence Integrated Intensity Measurements. The kinetics of both unfolding and refolding were followed by fluorescence using an Applied Photophysics DX-17MV stopped-flow spectrophotometer. Fluorescence measurements were made by exciting at 290 nm (2.5 nm band-pass) via a 0.2 cm path length and monitoring the emission intensity above 305 nm at 90° with a WG305 Schott glass filter (Oriel) at 25 °C. For both unfolding and refolding experiments, 2.5 and 0.5 mL drive syringes were employed to mix 5 parts of denaturant solution with 1 part of protein solution (1.56 mg/mL) for final urea concentrations ranging from 0.33 to 8.0 M at a final protein concentration of 0.26 mg/mL. The deadtime for this instrument under these mixing conditions was determined using the reaction of *N*-bromosuccinimide (NBS) with *N*-acetyltryptophanamide (NATA) (Peterman, 1979). The deadtime ranged between 5 and 10 ms, with the highest values occurring for the largest changes in denaturant concentration. Data collected during the deadtime were discarded from the analysis.

The nonlinear least-squares regression program supplied by Applied Photophysics was used to determine the best fit of these kinetic data to the rate equation:

$$A(t) = \sum^{i} A_i \exp(-k_i t) + A_\infty \qquad (1)$$

where A(t) is the amplitude of the change at time t, A_∞ is the amplitude at infinite time, A_i is the amplitude at zero time of phase i, and k_i is the rate of phase i. Goodness of fit to the various models was assessed by the criteria of Mannervik (1982) and Motulsky and Ransas (1987). Initial fitting was to a monophasic decay equation ($i = 1$). Additional phases were added to the equation until no significant improvement in the residual sum of squares was observed.

Wavelength-Dependent Stopped-Flow Fluorescence. The Applied Photophysics DX-17MV stopped-flow apparatus was adapted for the study of time-dependent fluorescence spectral changes by replacing the WG305 cutoff filter with a high-efficiency monochromator. Kinetic time courses (1000 data points) depicting the change in intensity during unfolding or refolding were collected for each 10 nm interval over a wavelength range from 310 to 400 nm with a band-pass of 9.3 nm. The excitation wavelength and band-pass were 290 nm and 9.3 nm, respectively. For both unfolding and refolding experiments, 5 parts of denaturant was mixed with 1 part of protein solution (3.12 mg/mL) in the buffer

described above. Final urea concentrations were 5.6, 6.8, and 7.7 M for unfolding studies and 1.2, 2.0, and 3.0 M for refolding experiments. The final protein concentration was 0.52 mg/mL.

The GLINT software package provided by Applied Photophysics was used to analyze the complete spectral data set. This program allows the entry of models that describe potential reaction mechanisms, the initial concentration of the reactants, and globally optimizes the kinetic rates and amplitudes that describe the transition at each wavelength by nonlinear least-squares regression. Finally, the program fits by numerical integration the spectra and concentration of the reactants, intermediates, and products that participate in the reaction. At completion, the program produces goodness of fit parameters and residual plots of the kinetic data at all wavelengths and times in order to determine the global accuracy of the model. As is true for all modeling methods to analyze kinetic data, the simplest model that provides a good fit to the data is considered to be the best model, but does not prove that the model is correct. The criteria of Mannervik (1982) and Motulsky and Ransas (1987) were used to assess the goodness of the fit.

The reaction of NBS with NATA (Peterman, 1979) was used to test the performance of the stopped-flow fluorometer in the spectral mode. The concentration of NATA was determined spectrophotometrically, and this concentration was used to determine the NBS concentration. Initially, 1 part of a 125 μM solution of NATA in 9 M urea in the buffer described above was mixed with 5 parts of a solution containing 200 μM NBS in buffer. The final concentrations of NATA, NBS, and urea were 25 μM, 167 μM, and 1.5 M, respectively. Kinetic time courses (1000 data points) depicting the loss in intensity during this reaction were collected for each 10 nm interval over a wavelength range from 310 to 400 nm with a band-pass of 9.3 nm. The excitation wavelength and band-pass were 285 nm and 9.3 nm, respectively. This reaction appears to be first order under these conditions, and fit well to the same monophasic decay process at each wavelength, implying no spectral or mixing artifacts are present. However, this reaction is more rapid than the rate of the normal protein unfolding or refolding transition, being complete in less than 50 ms. As such, the same reaction was performed at a slight excess of NBS (final concentration of NBS of 35 μM). Under these conditions, the reaction is second order, is complete in about 0.5 s, and as expected could not be fit by a simple monophasic decay. The GLINT software package fit the data well at all wavelengths to the simple model for a bimolecular reaction (Scheme 1) where A is NATA, B is NBS, and C is the nonfluorescent product of the reaction.

Scheme 1

$$A + B \rightleftharpoons C$$

Stopped-Flow CD Measurements. An Applied Photophysics RX1000 stopped-flow instrument in conjunction with a Jasco J710 CD spectropolarimeter was used for these measurements. This stopped-flow instrument has a standard size cuvette attached via a thermostated umbilical to the drive and stop syringes. A $^3/_4$ in. diameter plano convex fused silica lens (Oriel) of focusing length 100 mm at 589 nm was used to focus the large collimated light beam generated by the JASCO instrument on the center of the stopped-flow cell in the center of the sample compartment. Access to the sample compartment was gained through the top, allowing the larger surface area 2 mm path length cell to be used. The deadtime of the instrument is approximately 20−30 ms (Ropson et al., 1992). Data were fit to mono- and biexponential decay equations by nonlinear least-squares regression using KaleidaGraph (Synergy Software) on Macintosh computers.

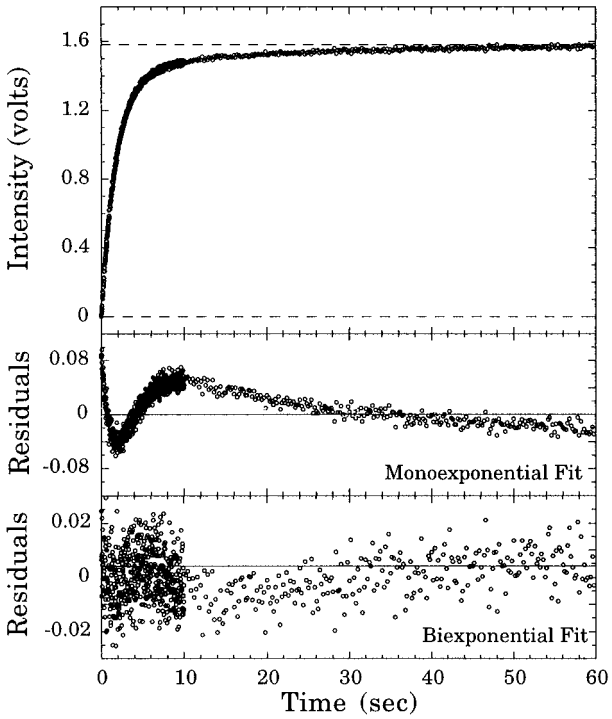

FIGURE 2: Change in the integrated fluorescence intensity vs time for the unfolding of IFABP. The final concentrations of urea and protein were 6.2 M and 0.26 mg/mL, respectively. The dashed lines are the values expected for completely folded and unfolded IFABP under these conditions. The residuals of the fit to a monophasic and biphasic relaxation equation are shown below the time course.

RESULTS

Integrated Stopped-Flow Fluorescence. A typical experiment showing the unfolding of IFABP as monitored by the integrated fluorescence at wavelengths greater than 305 nm is shown in Figure 2. The complete amplitude of the expected change in fluorescence was observed, as shown by the base line fluorescence levels expected for unfolded and folded protein under these conditions. More than one kinetic phase was observed for this transition, as shown by the greatly improved fit of the data to a biexponential decay (Figure 2). Similar results were found for all unfolding transitions at final concentrations of denaturant that cause the complete unfolding of IFABP. The faster phase was responsible for about 75−85% of the total amplitude change, with the remainder associated with the slower phase. Unfolding with guanidine hydrochloride resulted in biphasic unfolding kinetics as well (Ropson et al., 1990). A biphasic transition was also found when the transition was monitored by the absorbance change at 295 nm (data not shown). However, the small overall absorbance change prevented the accurate and consistent calculation of the amplitudes of these phases.

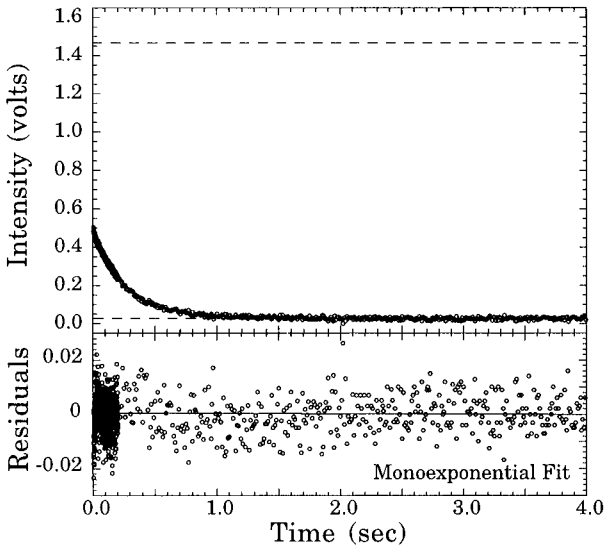

FIGURE 3: Change in the integrated fluorescence intensity vs time for the refolding of IFABP. The final concentrations of urea and protein were 2.2 M and 0.26 mg/mL, respectively. The dashed lines are the values expected for completely folded and unfolded IFABP under these conditions. The residuals of the fit to a monophasic relaxation equation are shown below the time course.

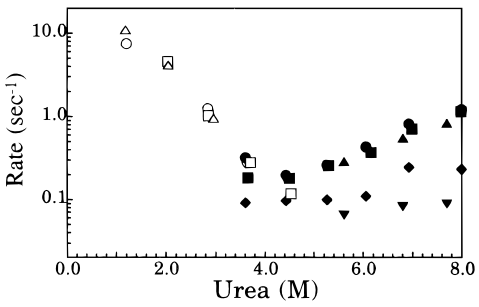

FIGURE 4: Rate constants for the folding and unfolding of IFABP. (●, ◆) The faster and slower rates for unfolding observed by the integrated stopped-flow fluorescence method. (▲, ▼) The faster and slower rates for unfolding by the spectral stopped-flow fluorescence method. (■) The single rate observed for unfolding by stopped-flow CD. (○, □, △) The single rate observed for refolding by integrated stopped-flow fluorescence, stopped-flow CD, and stopped-flow spectral methods, respectively.

During refolding, a significant amount of the expected amplitude was missing, as shown by the base line fluorescence levels expected for unfolded and folded protein under these conditions (Figure 3). The remaining fluorescence change was best fit by a monoexponential equation. The rate for this monophasic refolding phase was similar to that of the faster of the two rates during unfolding. At lower final concentrations of urea, more of the expected amplitude change occurred in the deadtime of mixing, although the remaining fluorescence change was still best fit to a monoexponential equation. The dependence of the rates of folding and unfolding on denaturant concentration is shown in Figure 4. These reaction rates were independent of final protein concentration over a range of 0.1−1 mg/mL (data not shown).

Stopped-Flow CD. The unfolding of IFABP by stopped-flow CD in the far-UV is shown in Figure 5A. During unfolding, a monophasic decay equation best fit the data for each transition monitored by CD, and the amplitude associated with this rate accounted for the entire expected amplitude change for the loss of secondary structure at that

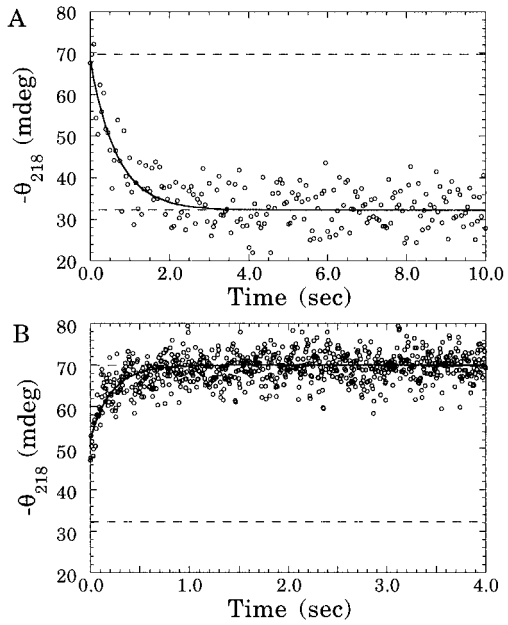

FIGURE 5: (A) Change in the circular dichroism signal at 218 nm during the unfolding of IFABP. The final concentrations of urea and protein were 6.2 M and 0.5 mg/mL, respectively. The line through the data is the fit to a monoexponential equation. (B) Change in the circular dichroism signal at 218 nm during the refolding of IFABP. The final concentrations of urea and protein were 2.0 M and 0.5 mg/mL, respectively. The line through the data is the fit to a monoexponential equation. The dashed lines represent the base line values for completely folded and unfolded protein under these conditions.

concentration of urea, as shown by the base line CD levels for unfolded and folded protein under these conditions. The same behavior was observed at other wavelengths (data not shown). The rates estimated by CD were identical to the faster of the two rates observed by fluorescence (Figure 4). Since the raw data for the stopped-flow CD transitions were noisy (Figure 5A,B), it is impossible to absolutely prove the complete absence of a second slower phase corresponding to the second fluorescence phase. However, it is clear that the amplitude of such a phase must be small compared to the total change, or it would have been detected. If the rates for a biphasic CD change were fixed to the values found for the fluorescence transition for a particular final denaturant concentration, less than 10% of the total amplitude change was assigned to the second slower rate, the error in the amplitude of the slower phase overlapped 0, and the residual sum of squares was not significantly improved over the monophasic fit. As such, it appears that no significant CD change occurs at the second slower rate.

A monophasic transition was observed by stopped-flow CD during refolding as well (Figure 5B), with a rate constant identical to that observed by fluorescence (Figure 4). A large part of the expected amplitude change occurred in the deadtime of mixing, similar to that described above for fluorescence during refolding. Lower final concentrations of urea again resulted in a larger amplitude for this burst phase.

Wavelength-Dependent Stopped-Flow Fluorescence. Figure 6A shows a subset (3% of the total collected data) of the emission fluorescence intensity at specific wavelengths during the unfolding of IFABP. The data are shown as spectral slices at individual time points. The transition was biphasic for individual wavelengths between 310 and 360

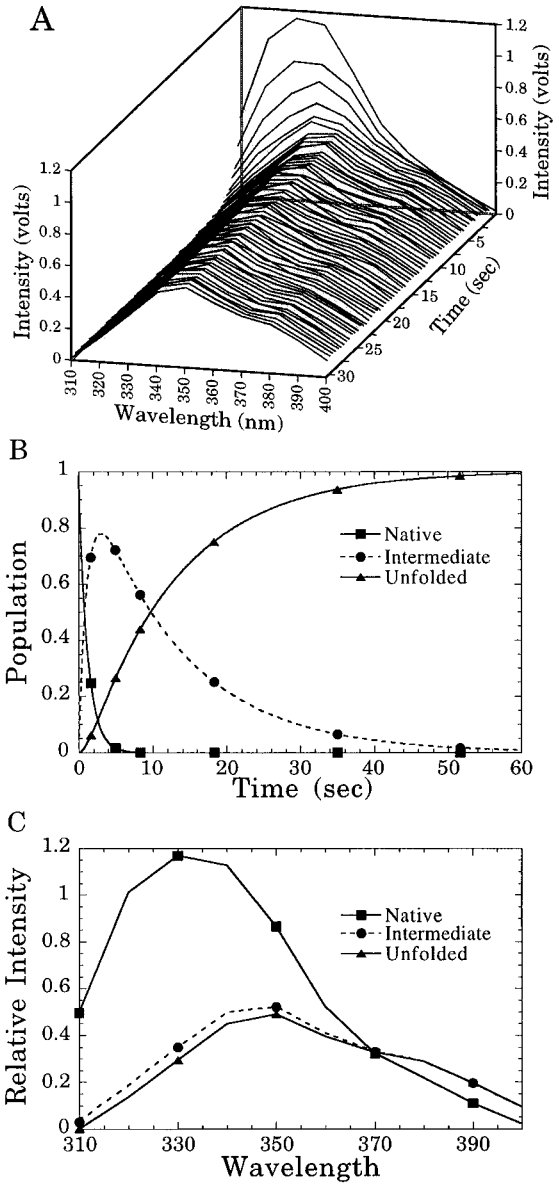

FIGURE 6: (A) Time-resolved fluorescence spectra for the unfolding of wild-type IFABP at a final concentration of 6.8 M urea and 0.52 mg/mL protein. Unfolding was initiated by mixing 1 part of native protein solution (3.1 mg/mL) in buffer containing 2.2 M urea, pH 7, with 5 parts of a 7.7 M urea solution in buffer. 1000 data points were collected at each wavelength. A portion of the data are presented as spectral slices at specific times after the initiation of unfolding. (B) Predicted time-dependent concentrations of each state from the fit of the model. (C) Predicted fluorescence spectra of the native, intermediate, and unfolded states of IFABP during unfolding.

nm, giving rates very similar to those observed by the integrated fluorescence experiments (Figure 4). Global analysis of these data at all wavelengths showed that the simplest model resulting in a good fit required the presence of an intermediate on the pathway for unfolding. The final concentration of denaturant was sufficient in these experiments such that this process could be considered an irreversible reaction. There was an initial rapid rise in the concentration of the intermediate, followed by the production of the unfolded species after an appreciable lag period (Figure 6B). The predicted initial spectra of the native, intermediate, and unfolded states are shown in Figure 6C. The initial and final spectra were identical to those expected for native and unfolded protein at this concentration of urea in this instrument. The intermediate spectrum was slightly more intense than that of the unfolded protein and may be slightly blue shifted compared to the spectrum of unfolded protein. However, this spectral shift was at the limit of resolution for this instrument under these conditions. Identical spectra for each conformation state were found for all unfolding transitions, although an increased rate of accumulation of the intermediate and unfolded species was observed at higher final concentrations of denaturant (Figure 4). These overall spectral changes would result in the biphasic unfolding kinetics observed by the integrated fluorescence change described above (Figure 2).

During refolding, the first observed spectrum was not identical to that of unfolded protein or the intermediate described above for the unfolding pathway (Figure 7A,C). This initial spectrum was between that of the native and unfolded protein (Figure 7C). A simple model describing a monophasic transition involving only an initial species and the final native species fit the data well. The rate of this transition was very similar to those observed during refolding by stopped-flow CD and integrated fluorescence experiments (Figure 4). When transitions were made to lower final concentrations of denaturant, the initial observed spectrum became still more native-like, with a further blue shift in the wavelength of maximal emission and a higher intensity (Figure 8). The final observed spectrum was identical to that expected for native protein at that concentration of denaturant in this instrument.

DISCUSSION

Historically, it has been easy to show that intermediates are present during the folding and unfolding of proteins by stopped-flow fluorescence experiments (Frieden et al., 1993; Engelhard & Evans, 1996). However, these reactions were monitored as total intensity changes, which do not inform the experimenter as to the nature of the intermediate involved. Further, there may be cases where a structural transition has occurred, as marked by a change in the wavelength of maximal emission, but no signal change is detected by stopped-flow fluorescence experiments because the overall integrated intensity does not change. The ability to obtain the fluorescence spectrum of protein folding intermediates will allow a better understanding of the structural nature of any protein folding intermediate. The wavelength of maximal emission for tryptophan provides a qualitative measure of the environment(s) of the tryptophan(s) in that structural state (Permyakov, 1993). Lower wavelengths of maximal emission (blue shifted compared to NATA in water) correspond to more hydrophobic environments. In the case of IFABP, there are two tryptophans, at positions 6 and 82 in the polypeptide chain (Figure 1). Both tryptophans are buried in the native state, with little solvent exposure. Presumably both tryptophans are equally solvent-exposed in the unfolded state. These measurements of changes in tryptophan environment during folding and unfolding can be combined with information on the rate of formation and breakdown of secondary structure by stopped-flow CD measurements in the far-UV. As such, improved hypotheses on the structural nature of the intermediate states found during the folding and unfolding of IFABP can be made.

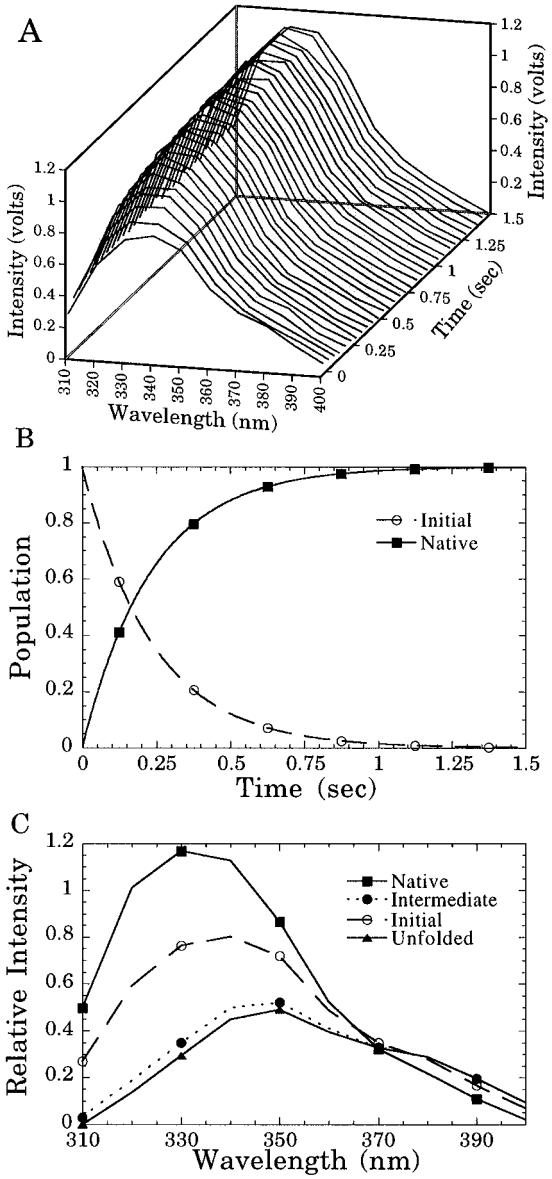

FIGURE 7: (A) Time-resolved fluorescence spectra for the refolding of IFABP at a final concentration of 2.0 M urea and 0.52 mg/mL IFABP. Refolding was initiated by mixing 1 part of unfolded protein (3.1 mg/mL) in buffer containing 7.0 M urea, pH 7, with 5 parts of a 1.0 M urea solution in buffer. 1000 data points were collected at each wavelength. A portion of the data are presented as spectral slices at specific times after the initiation of folding. (B) Predicted time-dependent concentrations of each state from the fit of the data to a simple two state model (I → N) where I is the initial state and N is the native state. (C) Predicted fluorescence spectra of the native and initial spectra are shown with the spectra of the intermediate and unfolded forms of IFABP from Figure 5 for comparison.

The Unfolding of IFABP. The presence of a kinetic intermediate during the unfolding of IFABP was unexpected. Most small, single-domain proteins like IFABP show monophasic kinetics during unfolding, suggesting that no detectable intermediate structures accumulate during unfolding (Goldenberg, 1988). As such, it is important to rigorously exclude the possibility that these observations are due to some artifact. Extensive tests were performed to exclude mixing artifacts (described under Materials and Methods). It is conceivable that the two kinetic phases observed are due to the presence of two different forms of the native protein, each having different unfolding rates. Since IFABP contains no prolines, proline isomerization cannot cause

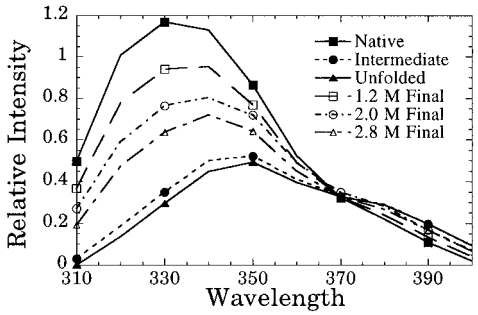

FIGURE 8: Initial observed spectra for the refolding of IFABP at several different final concentrations of denaturant. Refolding was initiated by mixing 1 part of unfolded protein (3.1 mg/mL) in buffer containing 7.0 M urea, pH 7, with 5 parts of buffer solutions containing 0 M, 1 M, or 2 M urea, resulting in the final concentration of urea being 1.2 M, 2.0 M, and 2.8 M, respectively. The spectra of the native, unfolded, and intermediate species observed during unfolding (Figure 5) are shown for comparison.

structural heterogeneity. Studies of the native apoprotein by two-dimensional NMR techniques have shown little structural heterogeneity in solution (D. Cistola, personnel communication). Another possible source of structural heterogeneity would be the presence of ligand on some of the protein molecules. The delipidation treatment of IFABP has been shown to be extremely effective, resulting in the removal of greater than 97% of all endogenous ligands (Lowe et al., 1987). Since IFABP binds ligands in a 1:1 molar ratio, less than 3% of the protein molecules have any ligand associated with them. Further, stopped-flow unfolding experiments were performed with protein containing bound oleate (1:1.1 molar ratio). This holoprotein also showed biphasic unfolding kinetics, with amplitudes for each of the phases similar to those shown for apoprotein (data not shown). Finally, several other members of this protein family also showed multiphasic unfolding transitions, implying that this phenomenon may be a common feature of this protein fold (data not shown). As such, it appears that the observed biphasic unfolding kinetics are not artifactual, but represent real structural transitions that occurred for all protein molecules during the unfolding of IFABP.

The clear superiority of the biphasic fit to the stopped-flow fluorescence transition (Figure 2) is most easily explained by the presence of an obligatory intermediate state during unfolding, as shown in Scheme 2.

Scheme 2

$$N \Longrightarrow I \Longrightarrow U$$

The model predicts a rapid loss of fluorescence intensity as the protein is converted from the native to the intermediate state, followed by a slower breakdown of the intermediate to the unfolded state. The stopped-flow CD transition for a given change in denaturant concentration had a rate identical to the transition from the native state to the intermediate state by fluorescence (Figure 4). The absence of the second phase by stopped-flow CD implies a lack of secondary structure for the intermediate. As such, this intermediate state is not a molten globule (Kuwajima, 1989), since no secondary structure was detected. To the best of our knowledge, this is the first case of a kinetic intermediate which lacks secondary structure during the unfolding of a protein.

The fluorescence spectra of each of the structural states are shown in Figure 5C. The fitted spectra of the native

and unfolded protein were identical to those measured at equilibrium for IFABP in this instrument, and very similar to those obtained in an Aminco Bowman Series 2 spectrofluorometer (data not shown). The slight increase in intensity at 380 nm for these spectra is due to a monochromator artifact. The spectrum of the intermediate was similar to that of the unfolded protein, although it was slightly more intense and may be slightly blue shifted. The tryptophans in this intermediate have similar environments to that of the unfolded state, but are not as quenched as in the unfolded protein when completely exposed to solvent. Considering the lack of secondary structure for this intermediate as shown by the stopped-flow CD experiments, it was not surprising that the fluorescence spectrum of the intermediate was so similar to that of unfolded protein. Higher final concentrations of urea increased the rates at which intermediate and unfolded protein were formed during unfolding, but did not change the shape of the observed spectra. Although this intermediate was treated as a single conformational state with a single unique fluorescence spectrum during the fitting process, there is likely to be a large family of similar conformational states present, each of which contributes to the overall fluorescence spectrum of the observed intermediate state.

This intermediate may have some fluctuating tertiary contacts that are the last remaining structure to unfold, after well-organized secondary structure has already been eliminated. Recent proton NMR studies of residual structure have shown the presence of both local and nonlocal hydrophobic tertiary contacts in proteins which appeared to be completely unfolded by optical techniques. This phenomenon has been observed for bovine pancreatic trypsin inhibitor (Pan et al., 1995; Lumb & Kim, 1994; Ittah & Haas, 1995), 434 repressor (Neri et al., 1992), and the α subunit of tryptophan synthase (Saab-Rincon et al., 1996).

Fluorine NMR studies of the folding transition of IFABP at equilibrium have shown that Trp-82 is involved in a conformational state in which Trp-6 does not participate (Ropson & Frieden, 1992). This equilibrium intermediate state also lacks secondary structure by CD criteria. It is tempting to suggest that only Trp-82 participates in this kinetic intermediate as well. This hypothesis is currently being tested with mutant proteins containing only a single tryptophan.

The Folding of IFABP. Refolding kinetics proved to be simpler in appearance but more difficult to interpret. During unfolding, the initial recorded spectrum was identical to that expected for native protein. However, during refolding, the initial recorded spectrum was significantly different from that of unfolded protein (Figure 7C). Therefore, the first observable species in solution immediately after mixing was not unfolded protein. Rather, some structural transition must have occurred to cause other specie(s) to be present, either instead of or in addition to the protein molecules still in the unfolded state. The remaining spectral changes fit simple monophasic decay kinetics. The observed rate was similar to that of the fast phase of unfolding and identical to the rate observed during refolding by the stopped-flow CD and integrated fluorescence experiments (Figure 4). Lower final concentrations of denaturant resulted in initial spectra more and more similar to that of native protein (Figure 8). These initial observed spectra were not similar to the fluorescence spectrum of the "molten globule like" form of IFABP that can be observed at equilibrium at pH 4 (data not shown). The presence of more native-like fluorescence spectra at lower concentrations of denaturant explains the increasing size of the burst phase amplitude change observed in the stopped-flow integrated fluorescence experiments. Stopped-flow CD experiments also showed an increasing burst phase amplitude during refolding of IFABP at lower concentrations of denaturant.

There are many possible interpretations of these results. One potential mechanism for this transition requires two different pathways for the folding of IFABP under strongly refolding conditions (Scheme 3).

Scheme 3

$$\text{refolding path 1: } U \Rightarrow N$$

$$\text{refolding path 2: } U \Rightarrow I \Rightarrow N$$

On the first pathway, some molecules fold to the native state very rapidly, in the deadtime of the instrument, resulting in native state fluorescence and CD for those molecules. On the other pathway, a population of molecules fold to the same intermediate state observed during unfolding in the deadtime of mixing, and then fold to the native state with monophasic kinetics similar to those of the fast phase of the fluorescence change observed during unfolding. Lower final concentrations of denaturant lead to more molecules following the faster folding pathway. For the data shown in Figure 7, about half the molecules were following the rapid pathway to the native state. Data from the folding of cytochrome *c* (Elöve et al., 1994; Sosnick et al., 1994), lysozyme (Kiefhaber, 1995), and ubiquitin (Khorasanizadeh et al., 1993) suggest that folding can occur via multiple pathways. For all of these proteins, the rapid folding path results in native structure for a portion of the protein molecules during the deadtime of mixing. In the case of ubiquitin, the proportion of molecules following a particular pathway is dependent on the solvent conditions (Khorasanizadeh et al., 1993).

Another simple mechanism compatible with the data places the species which causes the initial observed spectrum off the folding pathway (Miranker & Dobson, 1996) (Scheme 4).

Scheme 4

$$I^* \Leftrightarrow U \Leftrightarrow I \Rightarrow N$$

In this case, the I* structural state is some structure in rapid equilibrium with the unfolded state, but which does not lead to productive folding. Rather this conformation must unfold before the productive folding path can be taken. The I* state would have fluorescence and CD properties similar to those of the native state which would perturb the apparent initial spectrum as shown. The I state has a structure and fluorescence similar to those of the intermediate identified during unfolding, is also in rapid equilibrium with the unfolded state, and is an obligatory productive intermediate on the folding pathway.

These and other mechanisms for refolding are kinetically indistinguishable from each other with the data currently available (Miranker & Dobson, 1996). Further experiments by other methods are necessary to determine if any of these mechanisms are correct.

An understanding of the early steps in protein folding will require the combination of many different physical techniques to explore the structure of the early intermediates in this process (Engelhard & Evans, 1996). These experiments clearly show the utility of time-resolved spectral analysis in obtaining a better understanding of the nature of the intermediates that are formed during stopped-flow fluorescence experiments on the folding of IFABP.

ACKNOWLEDGMENT

We acknowledge the technical assistance of Susan Fromholt and thank Drs. C. Frieden, M. Fried, and D. P. Cistola for useful discussions of these data.

REFERENCES

Baldwin, R. L. (1993) *Curr. Opin. Struct. Biol. 3*, 84−91.
Creighton, T. E., Darby, N. J., & Kemmink, J. (1996) *FASEB J. 10*, 110−118.
Dill, K. A. (1990) *Biochemistry 29*, 7133−7155.
Dill, K. A., Fiebig, K. M., & Chan, H. S. (1993) *Proc. Natl. Acad. Sci. U.S.A. 90*, 1942−1946.
Dill, K. A., Bromberg, S., Yue, K., Fiebig, K. M., Yee, D. P., Thomas, P. D., & Chan, H. S. (1995) *Protein Sci. 4*, 561−602.
Elöve, G. A., Bhuyan, A. K., & Roder, H. (1994) *Biochemistry 33*, 6925−6935.
Engelhard, M., & Evans, P. A. (1996) *Folding Des. 1*, R31−R37.
Englander, S. W. (1993) *Science 262*, 848−849.
Englander, S. W., & Mayne, L. (1992) *Annu. Rev. Biophys. Biomol. Struct. 21*, 243−265.
Frieden, C., Hoeltzli, S. D., & Ropson, I. J. (1993) *Protein Sci. 2*, 2007−2014.
Goldenberg, D. P. (1988) *Annu. Rev. Biophys. Biophys. Chem. 17*, 481−507.
Gordon, J. I., Sacchettini, J. C., Ropson, I. J., Frieden, C., Li, E., Rubin, D. C., Roth, K. A., & Cistola, D. P. (1991) *Curr. Opin. Lipidol. 2*, 125−137.
Ittah, V., & Haas, E. (1995) *Biochemistry 34*, 4493−4506.
Johnson, W. C. (1988) *Annu. Rev. Biophys. Biophys. Chem. 17*, 145−166.
Khorasanizadeh, S., Peters, I. D., Butt, T. R., & Roder, H. (1993) *Biochemistry 32*, 7054−7063.
Kiefhaber, T. (1995) *Proc. Natl. Acad. Sci. U.S.A. 92*, 9029−9033.
Kuwajima, K. (1989) *Proteins: Struct., Funct., Genet. 6*, 87−103.
Kuwajima, K., Yamaya, H., Miwa, S., Sugai, S., & Nagamura, T. (1987) *FEBS Lett. 221*, 115−118.
Kuwajima, K., Sakuraoka, A., Fueki, S., Yoneyama, M., & Sugai, S. (1988) *Biochemistry 27*, 7419−7428.
LaLonde, J. M., Bernlohr, D. A., & Banaszak, L. J. (1994) *FASEB J. 8*, 1240−1247.
Levinthal, C. (1968) *J. Chim. Phys. 65*, 44−45.
Lowe, J. B., Sacchettini, J. C., Laposata, M., McQuillan, J. J., & Gordon, J. I. (1987) *J. Biol. Chem. 262*, 5931−5937.
Lumb, K. J., & Kim, P. S. (1994) *J. Mol. Biol. 236*, 412−420.
Mannervik, B. (1982) *Methods Enzymol. 87*, 370−389.
Matthews, C. R. (1993) *Annu. Rev. Biochem. 62*, 653−683.
Miranker, A. D., & Dobson, C. M. (1996) *Curr. Opin. Struct. Biol. 6*, 31−42.
Mo, J., Holtzer, M. E., & Holtzer, A. (1991) *Proc. Natl. Acad. Sci. U.S.A. 88*, 916−920.
Motulsky, H. J., & Ransnas, L. A. (1987) *FASEB J. 1*, 365−374.
Neri, D., Billeter, M., Wider, G., & Wuthrich, K. (1992) *Science 257*, 1559−1563.
Pace, C. N. (1986) *Methods Enzymol. 131*, 266−280.
Pan, H., Barbar, E., Barany, G., & Woodward, C. (1995) *Biochemistry 34*, 13974−13981.
Permyakov, E. A. (1993) *Luminescent Spectroscopy of Proteins*, CRC Press, Boca Raton, FL.
Peterman, B. F. (1979) *Anal. Biochem. 93*, 442−444.
Ptitsyn, O. B. (1996) *FASEB J. 10*, 3−4.
Ropson, I. J., & Frieden C. (1992) *Proc. Natl. Acad. Sci. U.S.A. 89*, 7222−7226.
Ropson, I. J., Gordon, J. I., & Frieden, C. (1990) *Biochemistry 29*, 9591−9599.
Ropson, I. J., Gordon, J. I., Cistola, D. P., & Frieden, C. (1992) in *Techniques in Protein Chemistry III* (Angeletti, R. A., Ed.) pp 437−443, Academic Press, New York.
Rose, G. D., & Wolfenden, R. (1993) *Annu. Rev. Biophys. Biomol. Struct. 22*, 381−415.
Saab-Rincon, G., Gualfetti, P. J., & Matthews, C. R. (1996) *Biochemistry 35*, 1988−1994.
Sacchettini, J. C., Banaszak, L. J., & Gordon, J. I. (1990) *Mol. Cell. Biochem. 98*, 81−93.
Sacchettini, J. C., Scapin, G., Gopaul, D., & Gordon, J. I. (1992) *J. Biol. Chem. 267*, 23534−23545.
Scapin, G., Gordon, J. I., & Sacchettini, J. C. (1992) *J. Biol. Chem. 267*, 4253−4269.
Sosnick, T. R., Mayne, L., Hiller, R., & Englander, S. W. (1994) *Struct. Biol. 1*, 149−156.
Sugawara, T., Kuwajima, K., and Sugai. S. (1991) *Biochemistry 30*, 2698−2706.
Veerkamp, J. H., & Maatman, R. G. H. J. (1995) *Prog. Lipid Res. 34*, 17−52.

BI962983B